Optica Applicata, Vol. XLI, No. 4, 2011

Optical properties of cross-linked chitosan thin film for copper ion detection using surface plasmon resonance technique

YAP WING FEN[1*], W. MAHMOOD MAT YUNUS[1], NOR AZAH YUSOF[2]

[1]Department of Physics, Faculty of Science, University Putra Malaysia, 43400 UPM Serdang, Selangor, Malaysia

[2]Department of Chemistry, Faculty of Science, University Putra Malaysia, 43400 UPM Serdang, Selangor, Malaysia

[*]Corresponding author: yapwingfen@gmail.com

The cross-linked chitosan is synthesized by homogeneous reaction of medium molecular weight chitosan in aqueous acetic acid solution with glutaraldehyde as cross-linking agent. Using surface plasmon resonance technique, the optical properties of cross-linked chitosan thin film before and after contacting with different concentrations of copper ion in a range of 0 to 100 ppm had been obtained by fitting. The imaginary part of refractive index increased while the thickness of the film decreased as copper ion concentration increased from 0 (deionised water) to 100 ppm. The resonance angle shifted to lower value as the copper ion concentration increased. By introducing the cross-linked chitosan film, copper ion detection can be obtained for concentration as low as 0.5 ppm using surface plasmon resonance technique.

Keywords: cross-linked chitosan, copper ion, surface plasmon resonance.

1. Introduction

Chitosan is a copolymer of glucosamine and *N*-acetylglucosamine linked by β-1, 4 glucosidic bonds. Chitosan occurs naturally in some microorganisms, yeast and fungi. It is a non-toxic, biocompatible and biodegradable natural polymer. The commercially available chitosan is mostly derived by alkaline *N*-deacetylation from chitin of crustaceans because it is easily obtained from the shells of crabs, shrimps, lobsters and krill. These two low-cost natural materials had been used for absorption of metal ions, dyes and protein. Compared to chitin, chitosan is more efficient in absorption capacity due to the presence of a large number of amino groups on chitosan chain. However, chitosan is soluble in organic acid, such as acetic acid and formic acid [1].

Cross-linking is an important step to improve the chemical stability of chitosan [2]. One cross-linking agent, glutaraldehyde, is an organic compound with the formula $CH_2(CH_2CHO)_2$. Glutaraldehyde is frequently used in biochemistry applications as an amine-reactive homobifunctional crosslinker.

In Malaysia, heavy metal pollution has grown to a dangerous level. This was proved based on a survey by the Department of Environment Malaysia which revealed that 4.9% of the 1 705 308.14 metric tonnes of schedule waste generated in 2009 contained heavy metal sludge [3]. One of the heavy metals, copper, in high doses can cause anemia, liver and kidney damage, and stomach and intestinal irritation. Different techniques for trace metal analysis including atomic absorption spectroscopy [4–9], inductively coupled plasma mass spectroscopy [10–14], electrochemical impedance spectroscopy [15, 16], voltammetry [17–20] and polarography [21, 22] have been widely used but these methods are expensive, complicated in sample treatment and mostly take a long measuring period. Optical sensor including surface plasmon resonance spectroscopy is an alternative and cost-effective method for this purpose [23].

Surface plasmon resonance (SPR) spectroscopy is a surface-sensitive technique [24] that has been used to characterize the thickness and refraction index of dielectric medium at noble metal surface [25]. For the last decade, surface plasmon resonance sensors have been extensively studied. Surface plasmon resonance technique has emerged as a powerful technique for a variety of chemical and biological sensor applications [26]. The first chemical sensing based on SPR technique was reported by LIEDBERG *et al*. (1983) [27]. SPR is an optical process in which light satisfying a resonance condition excites a charge-density wave propagating along the interface between a metal and dielectric material by monochromatic and *p*-polarized light beam [28]. The intensity of the reflected light is reduced at a specific angle of incidence producing a sharp shadow (called surface plasmon resonance) due to the resonance energy that occurs between the incident beam and surface plasmon wave [29]. SPR is regarded as a simple optical technique for surface and interfacial studies and shows great potential for investigating biomolecules [30]. SPR has been widely demonstrated as an effective optical technique for the study of interfaces and thin films [31]. A high specificity of the SPR optical sensor for heavy metal ions can be obtained by developing or depositing a thin layer of suitable material on gold thin film [32–39].

2. Theory

Surface plasmon wave propagates at the interface of two media with dielectric constant of opposite sign, *i.e.*, metal and dielectric. This surface plasmon wave is a TM-polarized wave (the electric field, E is parallel to the plane of incidence and perpendicular to the boundary surface between two media while the magnetic field B is perpendicular to the plane of incident and parallel to the boundary surface between two media) [40].

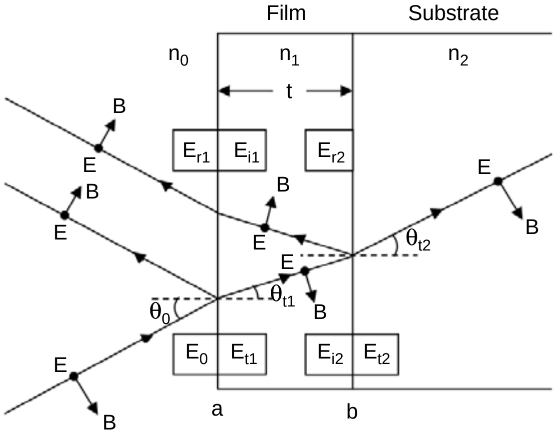

Fig. 1. Reflection of a beam from a single layer. The film thickness is represented by *t*. The insets define a terminology of *E* at the boundaries *a* and *b*. For example, E_{r1} represents the sum of all the multiple reflected beams at interface *a* in the process of emerging from the film, E_{i2} represents the sum of all the multiple beams incident at interface *b* and directed towards the substrate, and so on.

The magnitudes of magnetic field *B* and electric field *E* are related by

$$B = \frac{E}{v} \tag{1}$$

where the wave speed *v* is related to the refractive index *n* by

$$v = \frac{c}{n} \tag{2}$$

and the wave speed in vacuum *c* is a constant:

$$c = \frac{1}{\sqrt{\varepsilon_0 \mu_0}} \tag{3}$$

where ε_0 and μ_0 are the permittivity and permeability of free space, respectively.

By combining Eqs. (1), (2), and (3), the magnitudes of the magnetic field *B* and electric field *E* can be related by

$$B = \frac{E}{v} = \frac{n}{c}E = n\sqrt{\varepsilon_0 \mu_0}\, E \tag{4}$$

Based on Fig. 1 and by using Eq. (4) and the boundary conditions, the relationship between the magnetic and electric fields at the two interfaces can be written as follows:

$$B_a = n_0\sqrt{\varepsilon_0 \mu_0}\,(E_0 + E_{r1}) = n_1\sqrt{\varepsilon_0 \mu_0}\,(E_{t1} + E_{i1}) \tag{5}$$

$$B_b = n_1\sqrt{\varepsilon_0\mu_0}\,(E_{i2}+E_{r2}) = n_2\sqrt{\varepsilon_0\mu_0}\,E_{t1} \tag{6}$$

$$E_a = (E_0 - E_{r1})\cos(\theta_0) = (E_{t1} - E_{i1})\cos(\theta_{t1}) \tag{7}$$

$$E_b = (E_{i2} - E_{r2})\cos(\theta_{t1}) = E_{t2}\cos(\theta_{t2}) \tag{8}$$

By considering the phase change due to the light passing through different layers, *i.e.*,

$$E_{i1} = E_{r2}e^{-i\delta} \tag{9a}$$

$$E_{i2} = E_{t1}e^{-i\delta} \tag{9b}$$

$$B_{i1} = B_{r2}e^{-i\delta} \tag{9c}$$

$$B_{i2} = B_{t1}e^{-i\delta} \tag{9d}$$

and using the Euler identities, the relationships between E_1, B_1 and E_2, B_2 are obtained as follows:

$$E_a = \cos(\delta)E_b - \frac{i\sin(\delta)}{\gamma_1}B_b \tag{10}$$

$$B_a = -\gamma_1 i\sin(\delta)E_b + \cos(\delta)B_b \tag{11}$$

where

$$\gamma_1 = \frac{n_1}{\cos(\theta_{t1})}\sqrt{\varepsilon_0\mu_0} \tag{12}$$

Equations (10) and (11) may be written in matrix form as

$$\begin{bmatrix} E_a \\ B_a \end{bmatrix} = \begin{bmatrix} \cos(\delta) & -i\dfrac{\sin(\delta)}{\gamma_1} \\ -i\gamma_1\sin(\delta) & \cos(\delta) \end{bmatrix}\begin{bmatrix} E_b \\ B_b \end{bmatrix} \tag{13}$$

Thus, the transfer matrix for a single layer M_1 is:

$$M_1 = \begin{bmatrix} \cos(\delta) & -i\dfrac{\sin(\delta)}{\gamma_1} \\ -i\gamma_1\sin(\delta) & \cos(\delta) \end{bmatrix} \tag{14}$$

where δ is the phase shift due to the beam passing through different layers, *i.e.*,

$$\delta = \frac{2\pi}{\lambda}tn_1\cos(\theta_{t1}) \tag{15}$$

For the case of more than one layer, *i.e.*, the boundary *b* subtrate is replaced by the interface of another thin film, Eq. (13) is still valid. E_b and B_b are related to E_c and B_c at the back boundary of the second film layer by a second transfer matrix. Thus, for a multilayer film of arbitrary number *N* of layers,

$$\begin{bmatrix} E_a \\ B_a \end{bmatrix} = \prod_{i=1}^{N} M_N \begin{bmatrix} E_N \\ B_N \end{bmatrix} \tag{16}$$

The overall transfer matrix of the entire multilayer films, M_T can be represented in general by

$$M_T = \begin{bmatrix} m_{11} & m_{21} \\ m_{12} & m_{22} \end{bmatrix} \tag{17}$$

where m_{11}, m_{12}, m_{21} and m_{22} are the transfer matrix elements.

Based on Eqs. (5), (6), (7), (8) and (16), we obtain

$$\begin{bmatrix} (E_0 - E_{r1})\cos(\theta_0) \\ n_0\sqrt{\varepsilon_0\mu_0}\,(E_0 + E_{r1}) \end{bmatrix} = \begin{bmatrix} m_{11} & m_{21} \\ m_{12} & m_{22} \end{bmatrix} \begin{bmatrix} E_{t2}\cos(\theta_{t2}) \\ n_2\sqrt{\varepsilon_0\mu_0}\,E_{t1} \end{bmatrix} \tag{18}$$

After simplifying and making use of the reflection coefficient *r*, defined as

$$r = \frac{E_{r1}}{E_0} \tag{19}$$

we obtain

$$r = \frac{m_{21} + m_{22}\gamma_2 - m_{11}\gamma_0 - m_{12}\gamma_2\gamma_0}{m_{21} + m_{22}\gamma_2 + m_{11}\gamma_0 + m_{12}\gamma_2\gamma_0} \tag{20}$$

whereby the reflectivity *R* is

$$R = rr^* \tag{21}$$

Hence, a simulation and automatic fitting program have been developed using Matlab based on the matrix method as explained above.

3. Experiment

3.1. Materials

Chitosan with medium molecular weight and degree of deacetylation 75%–85% was purchased from Sigma Aldrich (St. Louis, MO, USA). Acetic acid and glutaraldehyde were also obtained from Aldrich. Standard solution of copper with concentration of 1000 ppm was purchased from Merck (Darmstadt, Germany).

A prism with refractive index $n = 1.7786$ at 632.8 nm and the substrate, glass cover slips 24×24 mm with thickness of 0.13–0.16 mm were purchased from Menzel-Glaser.

3.2. Preparation of copper ion solution

Copper ion standard solution (1000 ppm) was diluted by using dilution formula ($M_1V_1 = M_2V_2$) to produce copper ion solution with concentrations of 0.5, 1, 5, 10, 30, 50, 70 and 100 ppm.

3.3. Preparation of chitosan solution

To prepare chitosan solution, 0.40 g of chitosan was weighed and dissolved in 50 ml 1% acetic acid. The solution was stirred for 24 hours until all the chitosan was dissolved in acetic acid. Then, 0.05 g of glutaraldehyde was added to the solution to cross-link chitosan. The resulting solution was stirred for another 1 hour.

3.4. The pH measurement

The pH value of all the copper ion solutions was measured using a pH meter S20 (Mettler Toledo, Switzerland) with an attached combination pH electrode (LE428, Mettler Toledo, Switzerland).

3.5. Preparation of films

The glass cover slips were cleaned using acetone to clean off the dirt or remove fingerprint marks laid on the surface of glass slides. Then they were deposited with gold layer using an SC7640 Sputter Coater controlled by Film Thickness Monitor.

Spin coating technique was used to produce a thin layer of chitosan film on the top of the gold layer. Approximately 0.55 ml of the solution was placed on a glass cover slip covering the majority of the surface. The glass cover slip was spun at 6000 revolutions/min for 30 s using a Spin Coating System, P-6708D.

3.6. SPR system

Figure 2 shows the experimental setup for SPR measurement. The SPR measurement had been carried out by measuring the reflected He-Ne laser beam (632.8 nm, 5 mW)

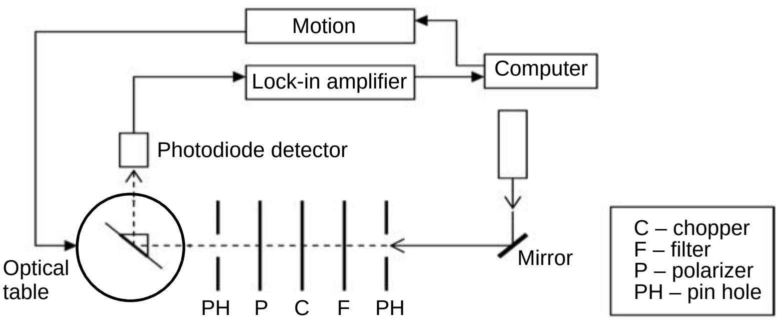

Fig. 2. Experimental setup for SPR measurement.

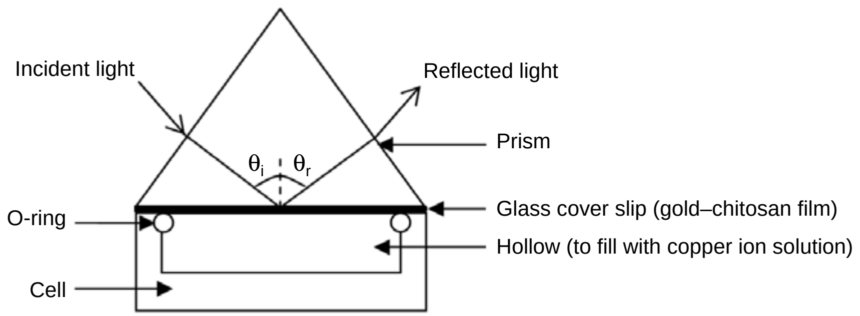

Fig. 3. Structure of the cell for SPR measurement.

as a function of angle of incidence. The optical set up consists of a He-Ne laser, an optical stage driven by a stepper motor with a resolution of 0.001° (Newport MM 3000), a light attenuator, a polarizer and an optical chopper (SR 540). The reflected beam was detected by a sensitive photodiode and then processed by the lock-in-amplifier (SR 530).

3.7. Sample cell

A cell was constructed to hold copper ion solution and make it come into contact with glass cover slip with thin films, as shown in Fig. 3. An open-ended brass cylindrical cavity with O-ring seal was attached to glass cover slip, which was attached to the prism by using index matching liquid. The copper ion solution was filled in the hollow formed so that the laser light comes into contact with the solution. The prism and the cell were mounted on a rotating plate to control the angle of the incident light.

4. Results and discussion

Firstly, the preliminary SPR test was carried out for gold film being in contact with deionised water (single layer) to determine the optical properties of gold layer (the real part of refractive of index n, the imaginary part of refractive index k, the thickness d of

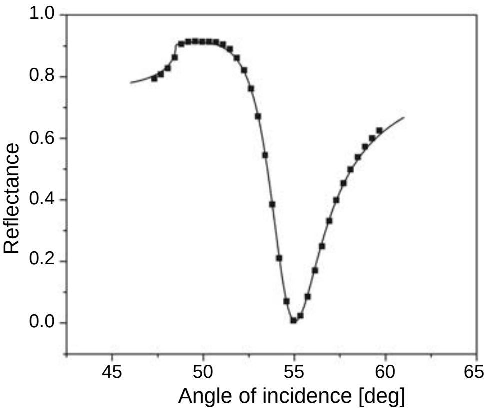

Fig. 4. Fitting experimental data to theoretical data for gold layer being in contact with deionised water. The solid line represents the theoretical curve.

the thin film) and deionised water. The experimental data and the fitted data are shown in Fig. 4. The optical properties of gold layer were obtained by using the developed Matlab fitting program (matrix method). The values of refractive index n and k, for gold layer are (0.190±0.005) and (3.305±0.002), respectively; the thickness d is (46.1±0.1) nm. The refractive index for deionised water is 1.3317. This information is important for further fitting of multilayer (gold/cross-linked chitosan) film.

The preliminary SPR test was also carried out for all concentrations (ranging from 0.5 to 1000 ppm) of copper ion solutions being in contact with gold film to determine

T a b l e 1. The real and imaginary parts of refractive index for different concentrations of copper ion solutions after fitting. (0 ppm represents deionised water.)

Concentration of copper ion [ppm]	Real part of refractive index n (±0.0005)	Imaginary part of refractive index k (± 0.0002)
0	1.3317	0
0.5	1.3318	0.0003
1	1.3318	0.0003
5	1.3318	0.0005
10	1.3318	0.0009
30	1.3319	0.0015
50	1.3319	0.0023
70	1.3319	0.0030
100	1.3321	0.0042
500	1.3351	0.0080
700	1.3366	0.0093
1000	1.3381	0.0108

T a b l e 2. The SPR resonance angle and shift of resonance angle for different concentrations of copper ion solutions being in contact with gold layer. (0 ppm represents deionised water.)

Concentration of copper ion [ppm]	Resonance angle θ_{min} [degree]	Shift of resonance angle $\Delta\theta$ [degree]
0	55.043	0
0.5	55.043	0
1	55.043	0
5	55.043	0
10	55.043	0
30	55.043	0
50	55.043	0
70	55.043	0
100	55.071	0.028
500	55.267	0.224
700	55.378	0.335
1000	55.490	0.447

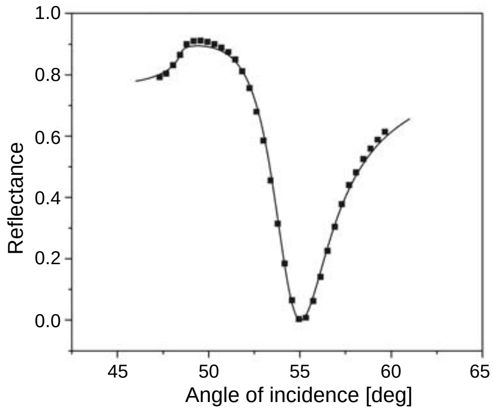

Fig. 5. Fitting experimental data to the theoretical data for gold layer being in contact with 50 ppm copper ion solution. The solid line represents the theoretical curve.

the refractive index of the solutions. All the results are tabulated in Tabs. 1 and 2. Figure 5 shows one typical graph for the experimental SPR curve fitted with theoretical data for gold layer being in contact with a 50 ppm copper ion solution. The SPR curves for copper ion solutions (100 to 1000 ppm) being in contact with gold layer are shown in Figs. 6 and 7.

The results showed that the shift of resonance angle is zero for low copper ion concentration below 100 ppm. Also, the real part of refractive index in this range of concentration is almost similar. This is probably due to the fact of only a small number of copper ion existing in these low concentration solutions to be adsorbed to gold surface. For high copper ion concentration (100 ppm and above), we believe that it is the increment in the number of ions adsorbed to gold surface that causes the SPR parameter to change. At high concentration, the shift of resonance angle increases as

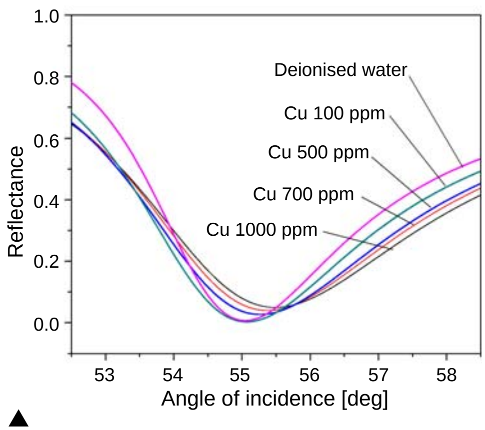

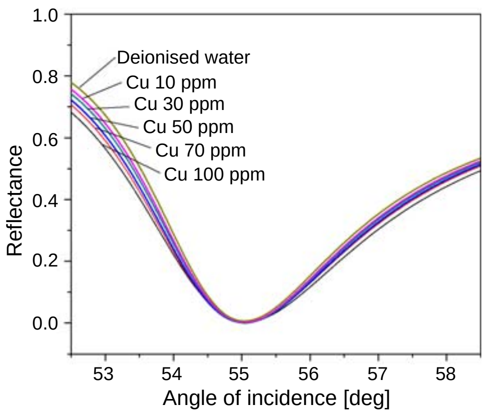

▲

Fig. 6. The SPR curves for copper ion solutions (100–1000 ppm) being in contact with gold layer.

Fig. 7. The SPR curves for copper ion solutions (10–100 ppm) being in contact with gold layer.

the copper ion concentration increases (as shown in Tab. 2 and Fig. 6), and the refractive indexes also increase with the copper ion concentration. Based on the above results, we are interested in increasing the sensitivity of SPR technique in detection of low copper ion concen-tration below 100 ppm.

Then, the SPR experiment was carried out for gold/cross-linked chitosan film being in contact with deionised water. The purpose of this procedure is to determine the optical properties of cross-linked chitosan layer (n, k and d). The experimental data and the fitted data are shown in Fig. 8. Using the multilayer Matlab fitting program, the properties of cross-linked chitosan thin film were determined, where $n = 1.540 \pm 0.005$, $k = 0.015 \pm 0.002$ and $d = 14.0 \pm 0.1$ nm.

The SPR experiment was carried out for copper ion solutions (0.5 to 100 ppm), which were injected one after another into the cell. Each injected solution was left for 10 minutes before the SPR curve was taken. All the fitting results for n, k and d are tabulated in Tab. 3 while the resonance angle and the shift of resonance angle for all

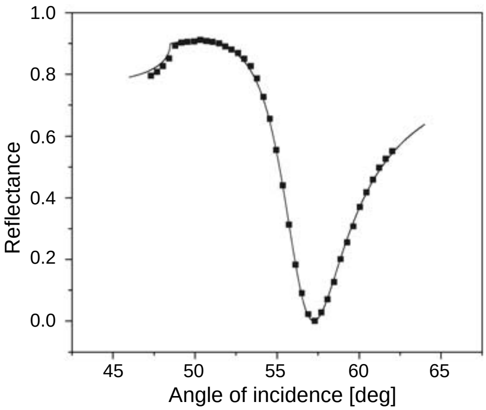

Fig. 8. Fitting experimental data to theoretical data for gold/cross-linked chitosan layer being in contact with deionised water. The solid line represents the theoretical curve.

Table 3. The real part and the imaginary part of refractive index, and the thickness for cross-linked chitosan film after fitting; with different concentrations of copper ion solutions injected into the cell (0 ppm represents deionised water).

Concentration of copper ion [ppm]	Real part of refractive index n (±0.005)	Imaginary part of refractive index k (±0.002)	Thickness of chitosan d (± 0.1) [nm]
0	1.540	0.015	14.0
0.5	1.540	0.022	13.9
1	1.540	0.023	13.9
5	1.539	0.026	13.9
10	1.538	0.035	13.7
30	1.536	0.040	13.1
50	1.534	0.055	12.3
70	1.532	0.071	11.4
100	1.530	0.099	10.1

T a b l e 4. The SPR resonance angle and the shift of resonance angle with different concentrations of copper ion solutions being in contact with gold/cross-linked chitosan layer (0 ppm represents deionised water).

Concentration of copper ion [ppm]	Resonance angle $\theta_{\min}$ [degree]	Shift of resonance angle $\Delta\theta$ [degree]
0	57.248	0
0.5	57.236	0.012
1	57.228	0.020
5	57.200	0.048
10	57.158	0.090
30	57.053	0.195
50	56.924	0.324
70	56.780	0.468
100	56.601	0.647

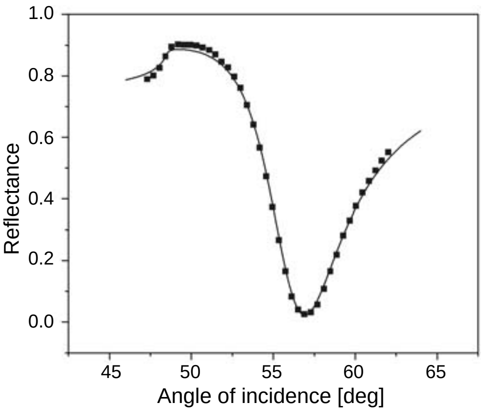

Fig. 9. Fitting experimental data to the theoretical data for gold/cross-linked chitosan layer being in contact with 50 ppm copper ion solution. The solid line represents the theoretical curve.

different concentrations of copper ion solution are shown in Tab. 4. Figure 9 shows one typical graph for the experimental SPR curve fitted with theoretical data for gold/cross-linked chitosan layer being in contact with a 50 ppm copper ion solution. The SPR curves for copper ion solutions (0.5 to 100 ppm) being in contact with gold/cross-linked chitosan layer are shown in Figs. 10 and 11.

The results show that the value of k for cross-linked chitosan layer increased as the concentration of copper ion increased. The thickness of the cross-linked chitosan layer decreased as the concentration of copper ion increased, most probably due to the shrinking of the sensor system.

The pH measurement showed that the values of pH of all copper ion solutions (0.5–100 ppm) were in the range between 5.9 to 6.5, *i.e.*, near to neutral pH value. This pH value was chosen and kept constant for all the SPR experiments as the adsorption of copper ion is optimum at this value [41]. This can be explained by the fact that at low pH (pH < 5), amine groups of chitosan are protonated, which induces an electrostatic repulsion of copper ion. As a result, the adsorption capacity is decreased. On

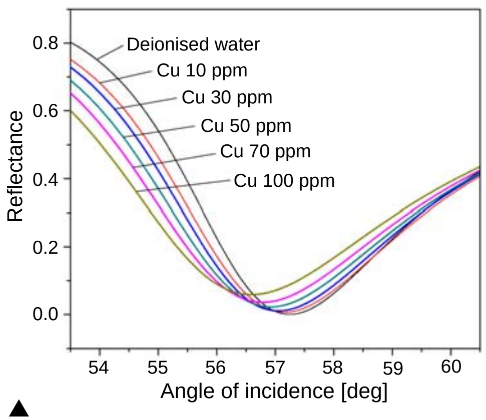

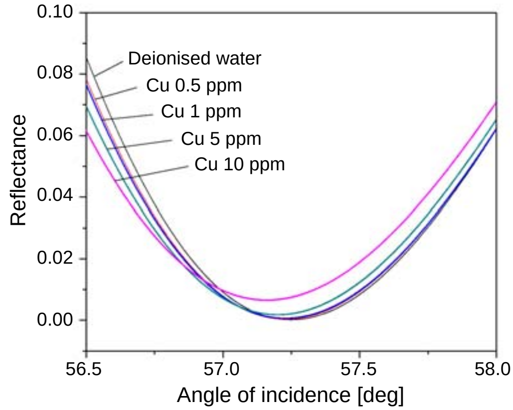

Fig. 10. The SPR curves for copper ion solutions (10–100 ppm) being in contact with gold/cross-linked chitosan layer.

Fig. 11. The SPR curves for copper ion solutions (0.5–10 ppm) being in contact with gold/cross-linked chitosan layer.

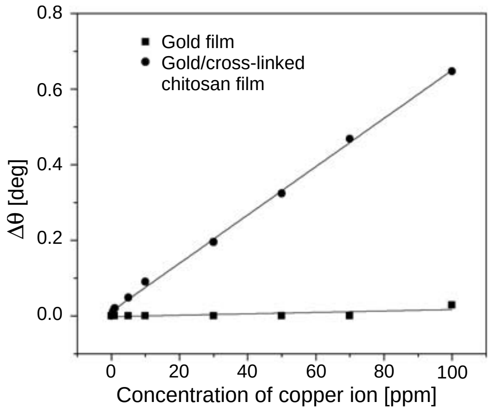

Fig. 12. Comparison of the shift of resonance angle for different concentrations of copper ions being in contact with gold film and gold/cross--linked chitosan film.

the other hand, at higher pH values (basic solution), precipitation of copper hydroxide occurs simultaneously with the adsorption of copper ion. The formation of copper hydroxide affects the adsorption by the cross-linked chitosan film.

In this study, we also proved that the cross-linked chitosan thin film had an important role in detection of copper ion. There were no changes in resonance angle for copper ion concentration below 100 ppm being in contact with gold only film. As the cross-linked chitosan thin film was introduced above gold layer, the resonance angle changed obviously and the detection limit determined was as low as 0.5 ppm. The difference is probably due to the fact of more copper ions interacting with cross--linked chitosan layer compared to gold only layer. A comparison of the shift of resonance angle for both gold film and gold/cross-linked chitosan film being in contact with different concentrations of copper ions is shown in Fig. 12.

5. Conclusions

In this work, the optical properties of cross-linked chitosan thin film with glutaraldehyde, before and after coming into contact with different concentrations of copper ions ranging from 0 to 100 ppm had been obtained using surface plasmon resonance technique. As the concentration increased from 0 (deionised water) to 100 ppm, the value of k increased while the thickness of the cross-linked chitosan film decreased. This led to the resonance angle shift to lower value as the copper ion concentration increased. Besides, the refractive index for different concentrations of copper ion solution were determined by making the solution to get into contact with gold only film. The results showed that there were no changes in resonance angle for copper ion concentration below 100 ppm. The cross-linked chitosan film had increased the sensitivity of the copper ion detection. The change in resonance angle was obtained for the copper ion concentration as low as 0.5 ppm.

Acknowledgements – The authors would like to thank the Malaysian Government for the fund support through SAGA. The laboratory facilities provided by the Department of Physics, Faculty of Science, University Putra Malaysia, are also acknowledged.

References

[1] SHAUER C.L., CHEN M.S., CHATTERLEY M., EISEMANN K., WELSH E.R., PRICE R.R., SCHOEN P.E., LIGLER F.S., *Color changes in chitosan and poly(allyl amine) films upon metal binding*, Thin Solid Films **434**(1–2), 2003, pp. 250–257.

[2] BHUMKAR D.R., POKHARKAR V.B., *Studies on effect of pH on cross-linking of chitosan with sodium tripolyphosphate: A technical note*, AAPS PharmSciTech **7**(2), 2006, article 50.

[3] *Malaysia Environmental Quality Report 2009*, Department of Environment, Ministry of Natural Resources and Environment, Malaysia, 2009, pp. 73–80.

[4] MAGEE R.J., RAHMAN, A.K.M., *Determination of copper in sea water by atomic absorption spectroscopy*, Talanta **12**(4), 1965, pp. 409–416.

[5] HOHNADEL D.C., SUNDERMAN F.W., NECHAY M.W., MCNEELY M.D., *Atomic absorption spectrometry of nickel, copper, zinc, and lead in sweat collected from healthy subjects during sauna bathing*, Clinical Chemistry **19**(11), 1973, pp. 1288–1292.

[6] MUZZARELLI R.A., ROCCHETTI R., *The determination of copper in sea water by atomic absorption spectrometry with a graphite atomizer after elution from chitosan*, Analytica Chimica Acta **69**(1), 1974, pp. 35–42.

[7] FREEDMAN J.H., PEISACH J., *Determination of copper in biological materials by atomic absorption spectroscopy: A reevaluation of the extinction coefficients for azurin and stellacyanin*, Analytical Biochemistry **141**(2), 1984, pp. 301–310.

[8] BANNON D.I., MURASHCHIK C., ZAPF C.R., FARFEL M.R., CHISOLM J.J., *Graphite furnace atomic absorption spectroscopic measurement of blood lead in matrix-matched standards*, Clinical Chemistry **40**(9), 1994, pp. 1730–1734.

[9] BANNON D.I., CHISOLM J.J., *Anodic stripping voltammetry compared with graphite furnace atomic absorption spectrophotometry for blood lead analysis*, Clinical Chemistry **47**(9), 2001, pp. 1703–1704.

[10] DRESSLER V.L., POZEBON D., CURTIUS A.J., *Determination of heavy metals by inductively coupled plasma mass spectrometry after on-line separation and preconcentration*, Spectrochimica Acta Part B: Atomic Spectroscopy **53**(11), 1998, pp. 1527–1539.

[11] GOOSSENS J., MOENS L., DAMS R., *Inductively coupled plasma mass spectrometric determination of heavy metals in soil and sludge candidate reference materials*, Analytica Chimica Acta **304**(3), 1995, pp. 307–315.

[12] LEE K.H., OSHIMA M., MOTOMIZU S., *Inductively coupled plasma mass spectrometric determination of heavy metals in sea-water samples after pre-treatment with a chelating resin disk by an on-line flow injection method*, Analyst **127**(6), 2002, pp. 769–774.

[13] KOBAYASHI K., KATSUYA Y., ABDULAH R., KOYAMA H., *Rapid and direct determination of selenium, copper, and zinc in blood plasma by flow injection-inductively coupled plasma-mass spectrometry*, Biological Trace Element Research **115**(1), 2007, pp. 87–93.

[14] MANEA S., LUCA R., PRODANA M., *Application of inductively coupled plasma-mass spectrometry to investigate the presence of trace metals in human tooth*, European Cells and Materials **16**(Supplement 5), 2008, p. 10.

[15] CHANG B.-Y., PARK S.-M., *Electrochemical impedance spectroscopy*, Annual Review of Analytical Chemistry **3**, 2010, pp. 207–229.

[16] JU M.J., HAYASHI K., TOKO K., YANG D.H., LEE S.W., KUNITAKE T., *A new electrochemical sensor for heavy-metal ions by the surface-polarization controlling method*, The 13th International Conference on Solid-State Sensors, Actuators and Microsystems, 2005, Digest of Technical Papers, TRANSDUCERS'05, Vol. 2, 2005, pp. 1876–1879.

[17] GUNKEL P., FABREI B., PRADO G., BALITEAU J.Y., *Ion chromatographic and voltammetric determination of heavy metals in soils. Comparison with atomic emission spectroscopy*, Analusis **27**(10), 1999, pp. 823–828.

[18] GUODONG LIU, YUEHE LIN, YI TU, ZHIFENG REN, *Ultrasensitive voltammetric detection of trace heavy metal ions using carbon nanotube nanoelectrode array*, Analyst **130**(7), 2005, pp. 1098–1101.

[19] ZENG A., LIU E., TAN S.N., ZHANG S., GAO J., *Stripping voltammetric analysis of heavy metals at nitrogen doped diamond-like carbon film electrodes*, Electroanalysis **14**(18), 2002, pp. 1294–1298.

[20] TVAROZEK V., REHACEK V., SHTEREVA K., NOVOTNY I., BRETERNITZ V., KNEDLIK C., SPIESS L., *Thin film voltammetric microsensor for heavy metal analysis*, 24th International Conference on Microelectronics, Vol. 1, 2004, pp. 189–191.

[21] KALVODA R., *Polarographic determination of adsorbable molecules*, Pure and Applied Chemistry **59**(5), 1987, pp. 715–722.

[22] KOÇAK S., TOKUŞOGLU Ö., AYCAN Ş., *Some heavy metal and trace essential detection in canned vegetable foodstuffs by differential pulse polarography (DPP)*, Electronic Journal of Environmental, Agricultural and Food Chemistry **4**(2), 2005, pp. 871–878.

[23] HOMOLA J., YEE S.S., GAUGLITZ G., *Surface plasmon resonance sensors: Review*, Sensors and Actuators B: Chemical **54**(1–2), 1999, pp. 3–15.

[24] TAO N.J., BOUSSAAD S., HUANG W.L., ARECHABALETA R.A., D'AGNESE J., *High resolution surface plasmon resonance spectroscopy*, Review of Scientific Instruments **70**(12), 1999, pp. 4656–4660.

[25] YUSMAWATI W.Y.W., CHUAH H.P., MAHMOOD M.Y.W., *Optical properties and sugar content determination of commercial carbonated drinks using surface plasmon resonance*, American Journal of Applied Science **4**(1), 2007, pp. 1–4.

[26] ZHANG H.Q., BOUSSAAD S., TAO N.J., *High-performance differential surface plasmon resonance sensor using quadrant cell photodetector*, Review of Scientific Instruments **74**(1), 2003, pp. 150–153.

[27] LIEDBERG B., NYLANDER C., LUNDSTRÖM I., *Surface plasmon resonance for gas detection and biosensing*, Sensors and Actuators **4**, 1983, pp. 299–304.

[28] KURIHARA K., SUZUKI K., *Theoretical understanding of an absorption-based surface plasmon resonance sensor based on Kretchmann's theory*, Analytical Chemistry **74**(3), 2002, pp. 696–701.

[29] HOMOLA J., *Surface Plasmon Resonance Based Sensor*, Springer, New York, 2006, p. 45.

[30] WU C.M., LIN L.Y., *Utilization of albumin-based sensor chips for the detection of metal content and characterization of metal–protein interaction by surface plasmon resonance*, Sensors and Actuators B: Chemical **110**(2), 2005, pp. 231–238.

[31] MELÉNDEZ J., CARR R., BARTHOLOMEW D., TANEJA H., YEE S., JUNG C., FURLONG C., *Development of a surface plasmon resonance sensor for commercial applications*, Sensors and Actuators B: Chemical **39**(1–3), 1997, pp. 375–379.

[32] SOONWOO CHAH, JONGHEOP YI, ZARE R.N., *Surface plasmon resonance analysis of aqueous mercuric ions*, Sensors and Actuators B: Chemical **99**(2–3), 2004, pp. 216–222.

[33] YINTANG ZHANG, MAOTIAN XU, YANJU WANG, TOLEDO F., FEIMENG ZHOU, *Studies of metal ion binding by apo-metallothioneins attached onto preformed self-assembled monolayers using a highly sensitive surface plasmon resonance spectrometer*, Sensors and Actuators B: Chemical **123**(2), 2007, pp. 784–792.

[34] JUNGWOO MOON, TAEWOOK KANG, SEOGIL OH, SURIN HONG, JONGHEOP YI, *In situ sensing of metal ion adsorption to a thiolated surface using surface plasmon resonance spectroscopy*, Journal of Colloid and Interface Science **298**(2), 2006, pp. 543–549.

[35] FORZANI E.S., FOLEY K., WESTERHOFF P., TAO N., *Detection of arsenic in groundwater using a surface plasmon resonance sensor*, Sensors and Actuators B: Chemical **123**(1), 2007, pp. 82–88.

[36] MIRKHALAF F., SCHIFFRIN D.J., *Metal-ion sensing by surface plasmon resonance on film electrodes*, Journal of Electroanalytical Chemistry **484**(2), 2000, pp. 182–188.

[37] SUGUNAN A., THANACHAYANONT C., DUTTA J., HILBORN J.G., *Heavy-metal ion sensors using chitosan-capped gold nanoparticles*, Science and Technology of Advanced Materials **6**(3–4), 2005, pp. 335–340.

[38] SU-MI LEE, SHIN-WON KANG, DONG-UK KIM, JIAN-ZHONG CUI, SUNG-HOON KIM, *Effect of metal ions on the absorption spectra and surface plasmon resonance of an azacrown indoaniline dye*, Dyes and Pigments **49**(2), 2001, pp. 109–115.

[39] CHING-MEI WU, LIH-YUAN LIN, *Immobilization of methallothionein as a sensive biosensor chip for the detection of metal ions by surface plasmon resonance*, Biosensors & Bioelectronics **20**(4), 2004, pp. 864–871.

[40] PEDROTTI F.L., PEDROTTI L.M., PEDROTTI L.S., *Introduction to Optics*, Third Edition, Pearson Education, San Fransisco, CA, 2007, pp. 476–479.

[41] WAN NGAH W.S., ENDUD C.S., MAYANAR R., *Removal of copper(II) ions from aqueous solution onto chitosan and cross-linked chitosan beads*, Reactive and Functional Polymers **50**(2), 2002, pp. 181–190.

Received January 1, 2011
in revised form March 27, 2011